

## Determination of Firing Times for the Stochastic Fitzhugh-Nagumo Neuronal Model

**Henry C. Tuckwell**

*tuckwell@b3e.jussieu.fr*

*Department of Mathematics, University of California, Irvine, CA 92697, U.S.A., and  
Laboratory for Visual Neurocomputing, Riken Brain Science Institute, Wako-shi,  
Saitama 351-0198, Japan*

**Roger Rodriguez**

*rodrig@cptsu2.univ-mrs.fr*

*Centre de Physique Théorique, CNRS, F13288 Marseille Cedex 9, France*

**Frederic Y. M. Wan**

*fwan@math.uci.edu*

*Department of Mathematics, University of California, Irvine, CA 92697, U.S.A.*

We present for the first time an analytical approach for determining the time of firing of multicomponent nonlinear stochastic neuronal models. We apply the theory of first exit times for Markov processes to the Fitzhugh-Nagumo system with a constant mean gaussian white noise input, representing stochastic excitation and inhibition. Partial differential equations are obtained for the moments of the time to first spike. The observation that the recovery variable barely changes in the prespike trajectory leads to an accurate one-dimensional approximation. For the moments of the time to reach threshold, this leads to ordinary differential equations that may be easily solved. Several analytical approaches are explored that involve perturbation expansions for large and small values of the noise parameter. For ranges of the parameters appropriate for these asymptotic methods, the perturbation solutions are used to establish the validity of the one-dimensional approximation for both small and large values of the noise parameter. Additional verification is obtained with the excellent agreement between the mean and variance of the firing time found by numerical solution of the differential equations for the one-dimensional approximation and those obtained by simulation of the solutions of the model stochastic differential equations. Such agreement extends to intermediate values of the noise parameter. For the mean time to threshold, we find maxima at small noise values that constitute a form of stochastic resonance. We also investigate the dependence of the mean firing time on the initial values of the voltage and recovery variables when the input current has zero mean.

## 1 Introduction

---

Following the first use of microelectrodes to observe the activity of individual neurons in the mammalian central nervous system, it was soon found that such activity was for the most part highly irregular and unpredictable (Burns, 1968). There have been proposed and analyzed many mathematical models whose aim is to provide quantitative theories of these phenomena (Softky & Koch, 1993; Stevens & Zador, 1998; Lee & Kim, 1999; Tuckwell, 1989, has a review of early modeling). In the past several years, there has been a vigorous renewed interest in such aspects of neuronal spiking activity, especially with regard to an understanding of information processing (Shadlen & Newsome, 1995; Konig, Engel, & Singer, 1996; Tiesinga, José, & Sejnowski, 2000).

There have been many experimental studies of the spike trains emitted by cortical cells in response to natural and artificial stimulation (Burns, 1968; Kreiter & Singer, 1996), but it is still uncertain which models reproduce experimental details (Softky & Koch, 1993; Plesser & Gerstner, 2000). Whereas many early studies of neuronal networks were based on the assumption that there are two possible states for each element of the network corresponding to a firing or nonfiring nerve cell, models have since become increasingly realistic and have begun to include physiological details of neurons, including synaptic currents of various kinds. Methods of research have included phase analysis, simulation, or numerical integration of systems of ordinary differential equations, as well as direct analytical approaches to problems involving stochastic model neurons with synaptic input. We have recently reported a reductionist method for nonlinear noisy single neurons and networks in which differential equations are solved for the first- and second-order moments of the model dynamical variables (Tuckwell & Rodriguez, 1998).

Although there has been considerable progress with mathematical analysis of the behaviors of model neurons, much of the research has involved simplified models. In this direction, there have been advances with classical one-dimensional models, but these have mainly been for linear integrate-and-fire models such as lead to the subthreshold potential being represented as an Ornstein-Uhlenbeck process (Plesser & Tanaka, 1997; Plesser & Gerstner, 2000). There have been only a few analytical studies including noise in nonlinear models such as the Fitzhugh-Nagumo system and the Hodgkin-Huxley system (Rodriguez, 1995; Tanabe & Pakdaman, 2001). Although several software routines are available to implement simulation studies of model neurons with both linear and nonlinear dynamics, as, for example, in Liley, Alexander, Wright, and Aldous (1999), it is always desirable to have results obtained using analytical approaches.

Using the theory of multidimensional (Markov) diffusion processes, we derive equations for the moments of random variables associated with the time to reach threshold in the Fitzhugh-Nagumo system. Although this sys-

tem does not have as firm a basis as conductance-based Hodgkin-Huxley type models, it is relatively simple and more directly amenable to analysis. We describe several methods of finding firing times by solving associated ordinary or partial differential equations, including approximations suitable for small and large values of the noise parameter. Comparison will be made with results obtained by simulating the stochastic Fitzhugh-Nagumo system directly. In a subsequent article, we will conduct a similar analysis of the original Hodgkin-Huxley equations. The approach that we use can be employed for any conductance-based model.

## 2 The Stochastic Fitzhugh-Nagumo System ---

The Fitzhugh-Nagumo (FN) system of two differential equations has been employed to provide insight into the more complex Hodgkin-Huxley system of four equations. It shares with the latter the properties of subthreshold responses, action potentials or spikes in response to suitable stimuli, and repetitive activity (periodic solutions) in certain ranges of stimuli. There are associated Hopf bifurcations at the parameter values associated with the end points of these ranges.

We study the following corresponding stochastic version of this model (Tuckwell, 1986, 1989; Feng & Brown, 2000) in which the components obey the following equations,

$$dX = [f(X) - Y + I]dt + \sigma dW \quad (2.1)$$

$$dY = b(X - \gamma Y)dt, \quad (2.2)$$

where  $X = X(t)$  is the “voltage” variable,  $Y = Y(t)$  is the “recovery” variable,  $W$  is a standard (zero mean, variance  $t$ ) Wiener process,  $\sigma$  is a constant determining the overall input noise level,  $I = I(t)$  is a deterministic input current (stimulus) that may be constant or time varying, and  $b$  and  $\gamma$  are positive constants. The function  $f$  is a cubic

$$f(x) = kx(x - a)(1 - x), \quad (2.3)$$

where  $0 < a < 1$ . Usually one takes  $a < 1/2$  in order to obtain suitable supra-threshold responses.

**2.1 Exact Equations for the Moments of the Time to a Threshold.** Let  $T(x, y)$  be the first exit time of the vector-valued process  $(X, Y)$  from an open set  $A$  in the phase-space for a starting point  $(x, y) \in A$ . Assuming that the stimulus  $I$  is constant so that the process is in fact temporally homogeneous, the theory of Markov diffusion processes (Tuckwell, 1976) yields the following partial differential equations (PDEs) for the first moment

$F(x, y) = E[T(x, y)]$  and for the second moment  $G(x, y) = E[T^2(x, y)]$ :

$$[f(x) - y + I] \frac{\partial F(x, y)}{\partial x} + b(x - \gamma y) \frac{\partial F(x, y)}{\partial y} + \frac{\sigma^2}{2} \frac{\partial^2 F(x, y)}{\partial x^2} = -1, \quad (2.4)$$

$$[f(x) - y + I] \frac{\partial G(x, y)}{\partial x} + b(x - \gamma y) \frac{\partial G(x, y)}{\partial y} + \frac{\sigma^2}{2} \frac{\partial^2 G(x, y)}{\partial x^2} = -2F(x, y), \quad (2.5)$$

with suitable boundary conditions on the boundary of the set  $A$ . The set  $A$  will be chosen as an open rectangle  $Q$  containing  $(x, y)$ . Since we are primarily interested in the time taken for the potential variable  $X$  to reach a threshold value  $\theta > 0$  from the resting value  $X(0) = 0$ , the rectangle is taken to be  $(-\alpha, \theta) \times (y_1, y_2)$ , where  $\alpha$  is positive. The usual boundary conditions for first exits from the open rectangle  $Q$  are that  $F$  and  $G$  vanish on its boundaries.

In order to facilitate numerical solution, we modify these boundary conditions, but in such a way that accurate values are still obtained for the moments. The condition that  $F$  and  $G$  vanish along the line  $x = \theta$  is retained. For the parameter ranges and initial values of interest, most exits of  $(X, Y)$  from  $Q$  occur through the line  $x = \theta$  and, for the values of  $Y(0)$  considered here, away from the lines  $y = y_1$  and  $y = y_2$ . As  $\alpha \rightarrow \infty$ , the paths are less influenced by the boundary condition at  $x = -\alpha$ , with nearly all exits occurring at  $x = \theta$  rather than  $x = -\alpha$ . Hence, one may use a reflecting condition  $F_x(-\alpha, \cdot) = 0$ , where the subscript denotes partial differentiation, instead of  $F(-\alpha, \cdot) = 0$ . The zero-derivative conditions  $F_y(\cdot, y_1)$  and  $F_y(\cdot, y_2)$  may similarly be employed. These zero-derivative conditions facilitate numerical solution of the differential equations by avoiding sharp boundary layers at these three edges of  $Q$  and correspond to the Euler boundary conditions in a variational formulation of the problem. The time to first threshold crossing or time to first spike from an initial rest point  $(0, y_0)$  is not the same as the interspike interval in nonlinear models and has first and second moments  $F(0, y_0)$  and  $G(0, y_0)$ , respectively, where  $y_0 \in (y_1, y_2)$ .

### 3 Methods of Solution

---

We have approached the solution of the moment equations in various ways. Approximate solutions can always be obtained by simulation, as described in the next section. However, accurate numerical solution of the moment equations is a useful and perhaps necessary check on simulation results, which are subject to sampling error. We have pursued the following methods of solution: (1) a simplified approach, which considers the single component process  $X$ ; (2) approximate solution of the PDEs 2.4 and 2.5 when  $\sigma$  is small; and (3) the solution of the PDEs when  $\sigma$  is large.

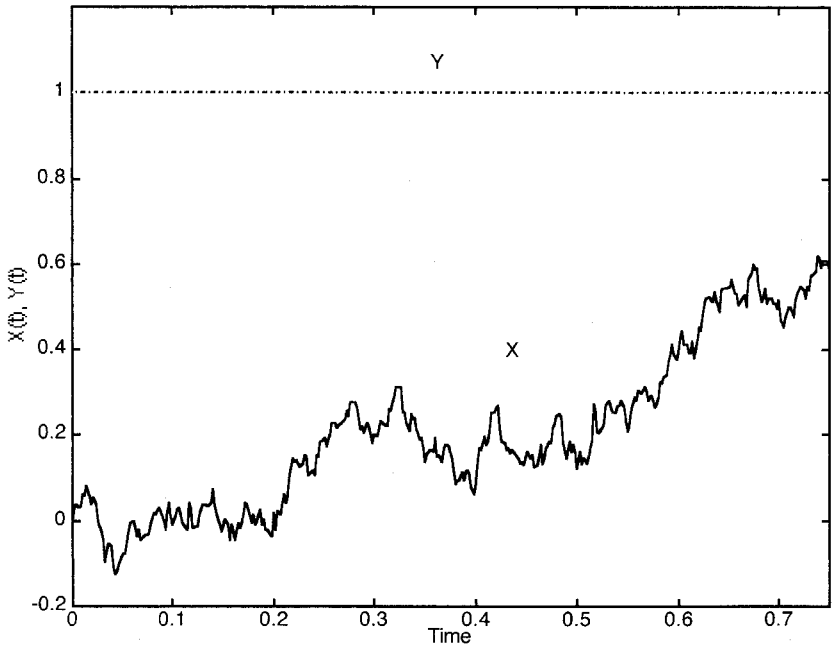


Figure 1: The value of the recovery variable is practically unchanged during the passage of  $X(t)$  from 0 to the threshold value of  $\theta = 0.6$ . Here the input current is  $I = 1.5$ , and the noise parameter is  $\sigma = 1$ . The values of the remaining parameters  $a = 0.1$ ,  $b = 0.015$ ,  $\gamma = 0.2$ ,  $k = 0.5$ , are the standard set throughout.

**3.1 A Simplified Approach.** In this first approach, we reduce the problem to a one-dimensional one. For the PDEs 2.4 and 2.5, this is tantamount to neglecting the  $F_y$  and  $G_y$  terms. The justification for this approach is the observation that during the initial stages of the interspike interval, the recovery variable  $Y(t)$  is practically unchanged and may therefore be set as a constant equal to the initial value  $Y(0) = y_0$ . This is illustrated in Figure 1.

We then consider the diffusion process satisfying

$$dX = [f(X) - y_0 + I]dt + \sigma dW. \quad (3.1)$$

Letting  $X(0) = x \in (-\infty, \theta)$ , we consider the exit time  $T_\theta(x)$ , which is the time to reach the level  $\theta$ , identified as the threshold for an action potential, given that the voltage started below this value. The first and second moments,  $F(x)$  and  $G(x)$ , respectively, of this exit time satisfy the differential equations

$$\frac{\sigma^2}{2} \frac{d^2 F(x)}{dx^2} + [f(x) - y_0 + I] \frac{dF(x)}{dx} = -1, \quad (3.2)$$

and

$$\frac{\sigma^2}{2} \frac{d^2 G(x)}{dx^2} + [f(x) - y_0 + I] \frac{dG(x)}{dx} = -2F(x), \quad (3.3)$$

with the boundary conditions  $F(\theta) = 0$  and  $G(\theta) = 0$ . For numerical solution, we make the interval of initial values finite with  $x \in (-\alpha, \theta)$ , where  $\alpha > 0$ . As mentioned in the previous section, at the lower boundary, it is advantageous to choose zero-derivative conditions  $F_x(-\alpha) = 0$  and  $G_x(-\alpha) = 0$ . The quantities of interest are the moments of the time to reach threshold from rest,  $F(0)$  and  $G(0)$ .

A further reduction is sometimes possible. The solutions of the second-order ordinary differential equations 3.2 and 3.3 may be approximated when  $\sigma$  is small by the solutions of the first-order equations

$$[f(x) - y_0 + I] \frac{dF(x)}{dx} = -1, \quad (3.4)$$

and

$$[f(x) - y_0 + I] \frac{dG(x)}{dx} = -2F(x). \quad (3.5)$$

These equations admit only a single boundary value, chosen as zero at  $x = \theta$ . A more accurate approach for small  $\sigma$  is described in the next section.

**3.2 Solution When  $\sigma$  Is Small.** When  $\sigma$  is small, the PDEs 2.4 and 2.5 can be solved approximately using perturbation methods. Putting  $\epsilon = \sigma^2/2$ , the equation satisfied by the mean first exit time can be written as

$$\epsilon F_{xx} + L_1[F] = -1, \quad (3.6)$$

with

$$L_1[F] = P(x, y)F_x + Q(x, y)F_y, \quad (3.7)$$

and where  $P(x, y) = I - y + kx(x - a)(1 - x)$  and  $Q(x, y) = b(x - \gamma y)$ . The solution is obtained with  $F(\theta, y) = 0$  and  $F_x(-\alpha, y) = 0$ . A regular perturbation expansion is sought in powers of  $\epsilon$ :

$$F(x, y; \epsilon) = \sum_{n=0}^{\infty} F_n(x, y) \epsilon^n. \quad (3.8)$$

Substitution in equation 3.6 gives first-order PDEs for the coefficients  $\{F_n(x, y)\}$ , which can be solved by the method of characteristics. For  $\sigma \ll 1$ , it is expected that the solution of equation 2.4 is

$$F(x, y; \epsilon) \approx F_0(x, y) + O(\epsilon),$$

where  $F_0$  is the leading term in the regular perturbation expansion, equation 3.8. A similar development leads to  $G(x, y; \epsilon) \approx G_0(x, y) + O(\epsilon)$ .

For the leading terms  $F_0$  and  $G_0$ , the relations 3.4 and 3.5 are applicable along with the characteristics of equations 2.4 and 2.5. Here, we have  $y = y_0(x)$ , known from a separate determination of the characteristic projections for the linear PDEs for  $F$  and  $G$ . It follows that the vanishing slope conditions for  $F$  and  $G$  as  $x \rightarrow -\infty$  are satisfied by  $F_0$  and  $G_0$ . For  $\sigma < 1$ , these leading term solutions (or the corresponding multiterm truncated perturbation series) differ by less than 5% from those obtained with the one-dimensional approach, validating the latter for such values of  $\sigma$ .

**3.3 Solution for Large  $\sigma$ .** It is convenient to rewrite equation 2.4 in dimensionless variables  $z = \frac{x}{\theta}$ ,  $\lambda = \frac{\sigma^2}{2\theta^2}$ , and  $u = \frac{y}{\theta}$ . The PDE becomes

$$\lambda F_{zz} + p(z, u)F_z + b(z - \gamma u)F_u = -1 \tag{3.9}$$

for  $-\bar{\alpha} \leq z \leq 1$ , where

$$p(z, u) = [\bar{I} + \bar{k}z(z - \bar{a})(1 - \theta z) - u] \tag{3.10}$$

and where  $\bar{I} = \frac{1}{\theta}$ ,  $\bar{k} = k\theta$ ,  $\bar{a} = \frac{a}{\theta}$ ,  $\bar{\alpha} = \frac{\alpha}{\theta}$ . The boundary conditions are now  $F(1, u) = 0$  and  $F_z(-\bar{\alpha}, u) = 0$ . With

$$\begin{aligned} P(z, u) &= \int^z p(w, u) dw \\ &= (\bar{I} - u)z + \bar{k} \left[ -\frac{\theta}{4}z^4 + \frac{1}{3}(1 + \theta\bar{a})z^3 - \frac{1}{2}\bar{a}z^2 \right], \end{aligned} \tag{3.11}$$

we multiply throughout by  $\frac{1}{\lambda}e^{P/\lambda}$  and write the PDE for  $F$  as

$$[e^{P/\lambda}F_z]_z + \frac{1}{\lambda}[b(z - \gamma u)e^{P/\lambda}F_u] = -\frac{e^{P/\lambda}}{\lambda}. \tag{3.12}$$

When  $\lambda \gg 1$ , a regular perturbation solution is sought of the form

$$F(z, u; \lambda) = \sum_{n=1}^{\infty} \bar{F}_n(z, u)\lambda^{-n}. \tag{3.13}$$

With the boundary conditions for the leading term given by  $\bar{F}_1(1, u) = 0$  and  $\bar{F}_{1,z}(-\alpha, u) = 0$ , the solution for  $\bar{F}_1$  can be found as a double integral. The following expression is then obtained for the mean first exit time:

$$F(z, u; \lambda) = \frac{1}{\lambda} \int_z^1 e^{-P(\eta, u)/\lambda} \int_{-\bar{\alpha}}^{\eta} e^{P(\zeta, u)/\lambda} d\zeta d\eta [1 + O(\lambda^{-1})]. \tag{3.14}$$

A similar analysis gives

$$G(z, u; \lambda) = \frac{1}{\lambda} \int_z^1 e^{-P(\eta, u)/\lambda} \int_{-\bar{a}}^\eta e^{P(\zeta, u)/\lambda} \bar{F}_1(\zeta, u) d\zeta d\eta \times [1 + O(\lambda^{-1})]. \quad (3.15)$$

In addition to yielding explicit accurate approximations for the moments of the first passage time, the above leading term asymptotic solutions (or more accurate multiterm truncated series solutions) provide, for large  $\sigma$ , validation of the one-dimensional approximation of section 3.1. The leading term of the perturbation solution for  $F$  is seen from equation 3.12 to be determined by equation 3.2. Similar remarks apply to  $G$ .

#### 4 Results and Comparison with Simulation

---

We have determined the first two moments of  $T(x, y)$  by the above methods. We have additionally simulated the processes described by the evolution equations 2.1 and 2.2 using a standard strong Euler method. The use of this scheme is straightforward and is vindicated in the existing problem by virtue of the close agreement of the simulation results and those obtained using the analytical framework. To apply this method, with  $X(k\Delta t)$  and  $Y(k\Delta t)$  approximated by  $X_k$  and  $Y_k$ , respectively, the simulation scheme consists of the recursive relations

$$X_{k+1} = X_k + [f(X_k) - Y_k + I]\Delta t + \beta\sqrt{\Delta t}N_k$$

$$Y_{k+1} = Y_k + b[X_k - \gamma Y_k]\Delta t,$$

where  $k = 0, 1, 2, \dots$  and  $\{N_k\}$  is a sequence of independent and identically distributed standard normal random variables, obtained from computer library routines. This was done principally with the set of parameter values  $a = 0.1, b = 0.015, \gamma = 0.2$ , and  $k = 0.5$  for various values of  $\sigma$  and  $I$ . The threshold value  $\theta$  for spikes was estimated from sample paths with allowance for the discrete nature of simulation. The value of  $\Delta t$  was pragmatically chosen between 0.00001 and .001, the value being determined in each case by requiring the minimum number of steps to threshold to be at least 20 and the maximum number several thousand.

The initial value of  $X(t)$  was set at 0 and that of  $Y(t)$  usually set at 1.0 in the results to be reported. Other values of  $Y(0)$  were nevertheless considered for comparison, some being reported in the final section. When  $I$  is less than about 1.3, the (expected) value of  $X(t)$  rarely attains the designated threshold value of  $\theta = 0.6$ . For the chosen parameters, we therefore consider mainly values of  $I \geq 1.3$ , although the value  $I = 0$  is discussed later in the article. The values of the noise parameter  $\sigma$  are chosen from 0.05 to 5.0. For small



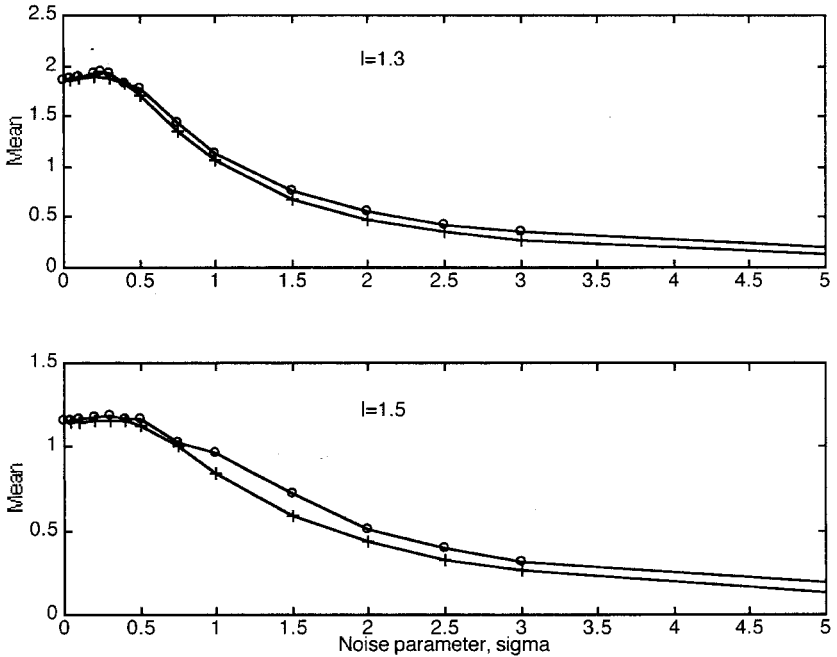


Figure 2: Mean times to reach threshold versus noise parameter  $\sigma$ . Parameter values are given in the text. Values are determined by simulation (circles) and by numerical solution of differential equation 2.4 (+).

values of  $\sigma$ , the number of trials in simulations was 4500, whereas only 1500 trials were employed for larger values.

Plots of the means of the times for  $X(t)$  to reach  $\theta$  for various  $I$  as a function of  $\sigma$  are shown in Figures 2 and 3. For a given value of  $I$ , results obtained by numerical solution are shown in the same figure for comparison. In Figure 2, the values of  $I$  are 1.3 and 1.5, whereas in Figure 3, the values of  $I$  are 2 and 3. The numerical results shown here were obtained using the simplified approach from section 3.1. There is excellent agreement between the two sets of results, especially allowing for sampling error in the simulation results. The magnitudes of sampling errors ( $\pm$  standard error) in the simulated means are summarized as follows, with best cases first. When  $I = 1.3$ , for  $\sigma = 0.05$ ,  $\pm 0.17\%$ ; for  $\sigma = 0.5$ ,  $\pm 1.31\%$ ; for  $\sigma = 0.75$ ,  $\pm 2.70\%$ ; and for  $\sigma = 5$ ,  $\pm 3.95\%$ . When  $I = 1.5$ , for  $\sigma = 0.05$ ,  $\pm 0.13\%$ ; for  $\sigma = 0.5$ ,  $\pm 1.20\%$ ; for  $\sigma = 0.75$ ,  $\pm 2.53\%$ ; and for  $\sigma = 5$ ,  $\pm 3.93\%$ . When  $I = 2$ , for  $\sigma = 5$ ,  $\pm 0.10\%$ ; for  $\sigma = 0.5$ ,  $\pm 0.92\%$ ; for  $\sigma = 0.75$ ,  $\pm 2.2\%$ ; and for  $\sigma = 5$ ,  $\pm 4.50\%$ . When  $I = 3$ , for  $\sigma = 0.05$ ,  $\pm 0.07\%$ ; for  $\sigma = 0.5$ ,  $\pm 0.66\%$ ; for  $\sigma = 0.75$ ,  $\pm 1.76\%$ ; and for  $\sigma = 5$ ,  $\pm 4.30\%$ .

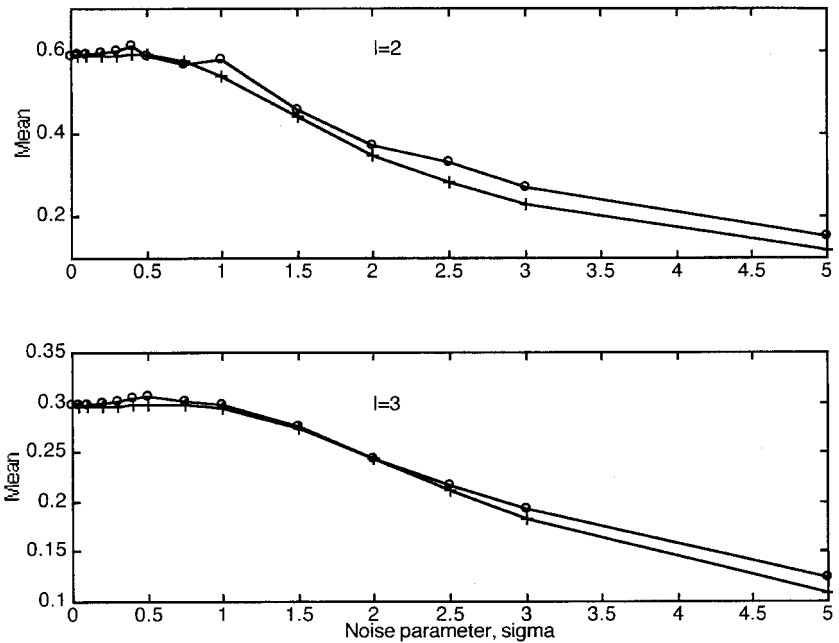


Figure 3: Mean first firing time versus  $\sigma$  when  $I = 2$  and  $I = 3$ . Values are determined by simulation (circles) and by numerical solution of differential equation 2.4 (+).

In general, the means from simulation are slightly larger than those obtained by solution of the differential equation. It can be clearly seen in the top part of Figure 2, where  $I = 1.3$ , that as  $\sigma$  increases away from zero, the mean first passage time actually increases. After reaching a maximum when  $\sigma$  is about equal to 0.25, the mean then declines, as is expected with increased variability. Similar behavior is observed for the larger values of the mean input current, except that the maximum of the mean interval occurs at larger values of  $\sigma$ . This phenomenon is akin to stochastic resonance, well documented in nonlinear systems with noise, including neural systems such as that of Hodgkin-Huxley and Fitzhugh-Nagumo (Lee & Kim, 1999; Nozaki & Yamamoto, 1998; Massanes & Vicente, 1999).

In Figures 4 and 5, we show the standard deviation of the time to reach threshold as determined by both simulation and solution of the differential equation 2.5 for the second moment. It can be seen that there is excellent agreement between the two sets of results for all four values of the input parameters  $I$  and  $\sigma$ . In each of the four sets of results shown, the standard deviation attains a maximum as a function of  $\sigma$ . The magnitudes of the sampling errors in the standard deviations in representative cases are as

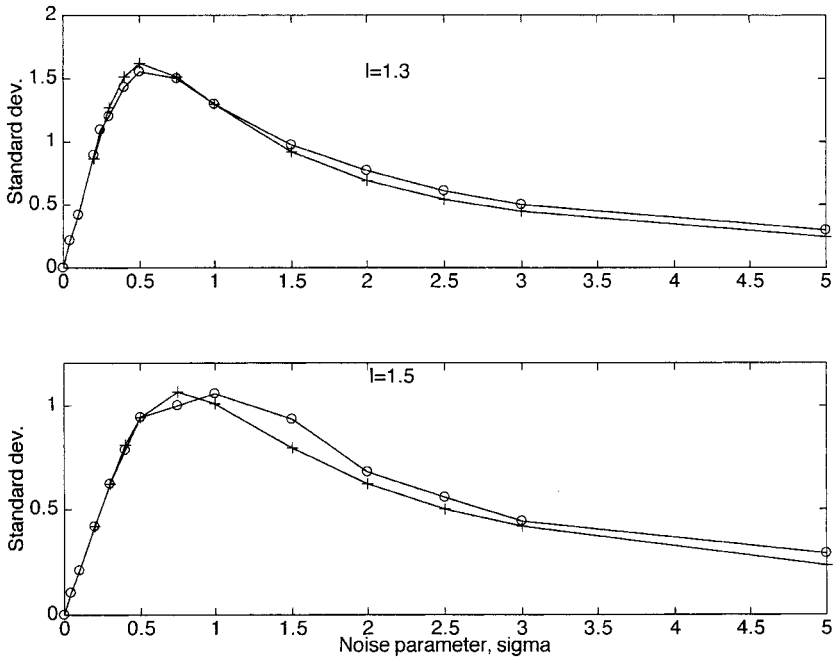


Figure 4: Standard deviation of time to reach threshold versus noise parameter  $\sigma$ . Parameter values are given in the text. Values are determined by simulation (circles) and by numerical solution (+) of the differential equation 2.4.

follows. When  $I = 1.3$ , for  $\sigma = 0.05$ ,  $\pm 2.0\%$ ; and for  $\sigma = 5$ ,  $\pm 2.6\%$ . When  $I = 3$ , for  $\sigma = 0.05$ ,  $\pm 2.2\%$ ; and for  $\sigma = 5$ ,  $\pm 4.8\%$ .

In Figure 6, we show the behavior of the coefficient of variation (CV, defined as standard deviation divided by the mean), calculated from computer simulations, as a function of the noise parameter  $\sigma$  for the values  $I = 1.3$  and  $I = 3$ . The results for  $I = 1.5$  and  $I = 2$  are similar to these, respectively. It is seen that the CV is greater than 1 over much of the range of parameters considered.

## 5 Discussion

Since interest first arose in the theory of stochastic neuronal firing over 30 years ago, analytical methods have been employed to determine properties of interspike intervals in many integrate-and-fire model neurons in which the subthreshold membrane potential satisfies a linear stochastic differential equation. In this regard, nonlinear models such as Fitzhugh-Nagumo and Hodgkin-Huxley have been studied mainly using computer simulations. We have used an analytical framework for the first time in a nonlinear

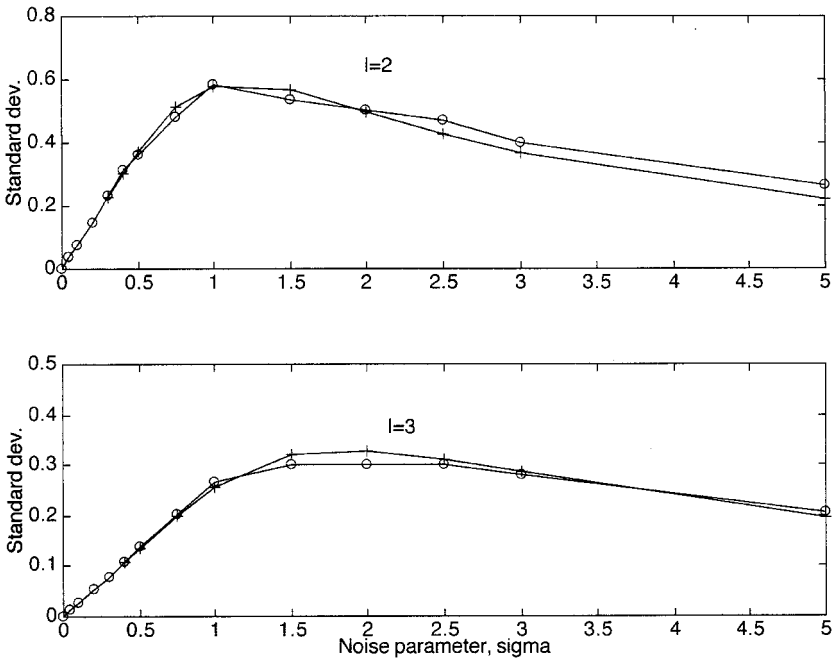


Figure 5: Standard deviation of first firing time versus  $\sigma$  when  $I = 2$  and  $I = 3$ . Values determined by simulation (circles) and by numerical solution of the differential equation 2.5 (+).

stochastic neural model. To this end, we have reduced the task of characterizing the firing time to the solution of linear second-order partial differential equations.

Some remarks about the nature of these equations and our methods of solution of them are in order when the noise term is small. In such singular perturbation problems, where the highest derivative term in the differential equation is multiplied by the small parameter, setting the small parameter equal to zero (or, equivalently, seeking the leading term of a regular perturbation solution in the small parameter) reduces the order of the equation and therefore leads to a loss of some of the components of the general solution of the equation. However, for problems with a certain combination of boundary conditions, such as prescribing the normal derivative equal to zero at negative infinity or at some large negative value of  $x$  and prescribing the value of the unknown (equal to zero in our case) at the opposite end of the interval, the missing solutions are irrelevant, as they would have been eliminated by the boundary condition at negative infinity anyway. That is, our less general solution, obtained after setting the small parameter  $\sigma$  equal to zero, is made to satisfy all boundary conditions (in particular, the

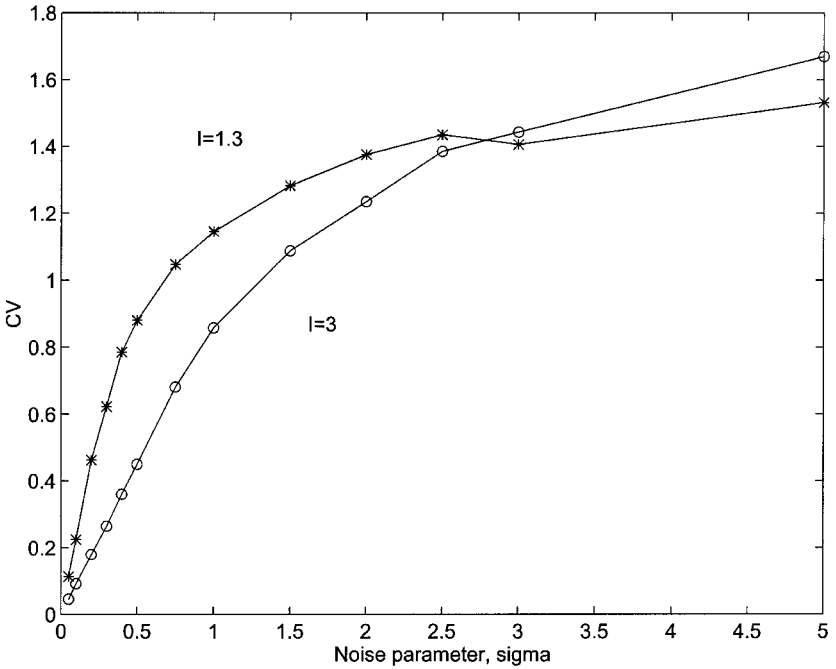


Figure 6: Coefficient of variation of the time to threshold versus  $\sigma$  for  $I = 1.3$  and  $I = 3$ . Values are determined by simulation (circles) and by numerical solution of the differential equation 2.5 (+).

condition at negative infinity automatically), whereupon by a uniqueness theorem for linear PDEs, we have the correct solution of the problem without obtaining the missing solutions. A previous example of this technique is contained in our extensive investigation of the Ornstein-Uhlenbeck process representation of neuronal potential (Wan & Tuckwell, 1982).

**5.1 Parameter and Initial Values: The Case  $I = 0$ .** The parameters we have employed are necessarily in restricted particular ranges, and a brief consideration of other cases is warranted. The deterministic constant component of the input current  $I$  represents the drift or the mean synaptic drive, which depends on the relative magnitudes and frequencies of excitation and inhibition. The quantities we have determined using an analytical framework are the moments of the time for emergence of the first spike. For values of  $I$  such as those employed in the calculations performed above, periodic firing occurs; that is, subsequent to the first spike, an approximately periodic spike train ensues. If the train is sufficiently regular with a consistently defined apparent threshold, such as occurs when the noise amplitude is not excessive (see Figure 2 of Tuckwell & Rodriguez, 1998), then the methods

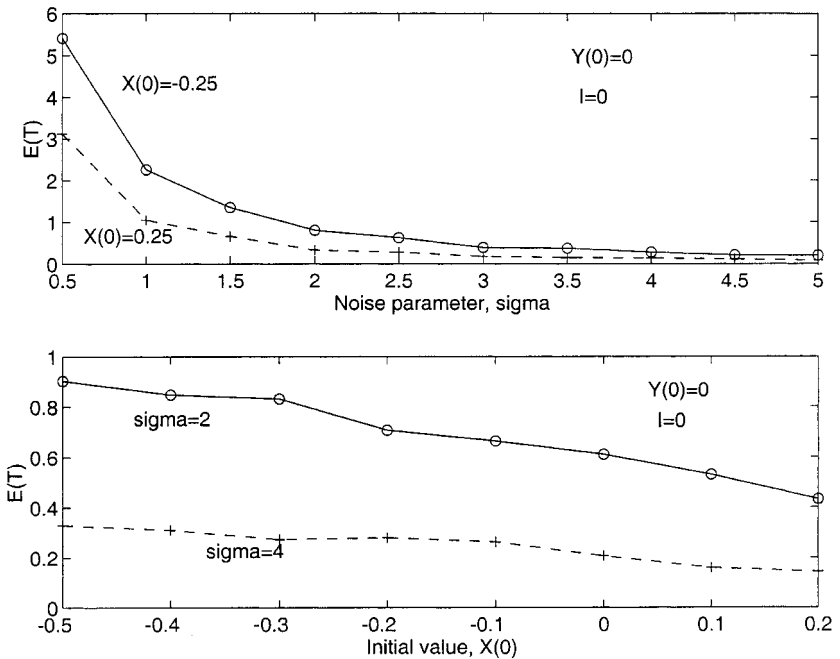


Figure 7: Effects of changing the initial value of the voltage variable  $X(0)$  are illustrated for a fixed value of  $Y(0) = 0$ . (Top) For the two indicated values of  $X(0)$ , the variation of the mean time to a spike as a function of noise parameter  $\sigma$  is shown. (Bottom) Variations in mean time to a spike as the initial value  $X(0)$  changes for two fixed values of the noise parameter.

employed here could be applied to the determination of the moments of the associated yet different random variable, namely, the interspike interval. Such a determination will be deferred to a later article.

The initial value chosen above for the dynamical variables  $X$  to illustrate the usefulness of the analytical approach is  $X(0) = 0$  because it corresponds to a natural resting or equilibrium value for the unperturbed system. The value  $Y(0) = 1$  was based on previously published results as it was close to the values in sustained rhythmic firing for chosen parameter values (Tuckwell & Rodriguez, 1998). However, other initial conditions are of interest and also the case where periodic firing does not necessarily occur because the mean input current is not sufficiently large.

To study these aspects, we have determined, using simulation, the statistics of the time to first spike in certain “excitable” cases when  $I = 0$ . First, we consider the effects of varying the initial value  $X(0)$  of the voltage variable for a fixed value  $Y(0) = 0$  of the recovery variable. Some results for the mean time to first spike are shown in Figure 7. Comparison of the results

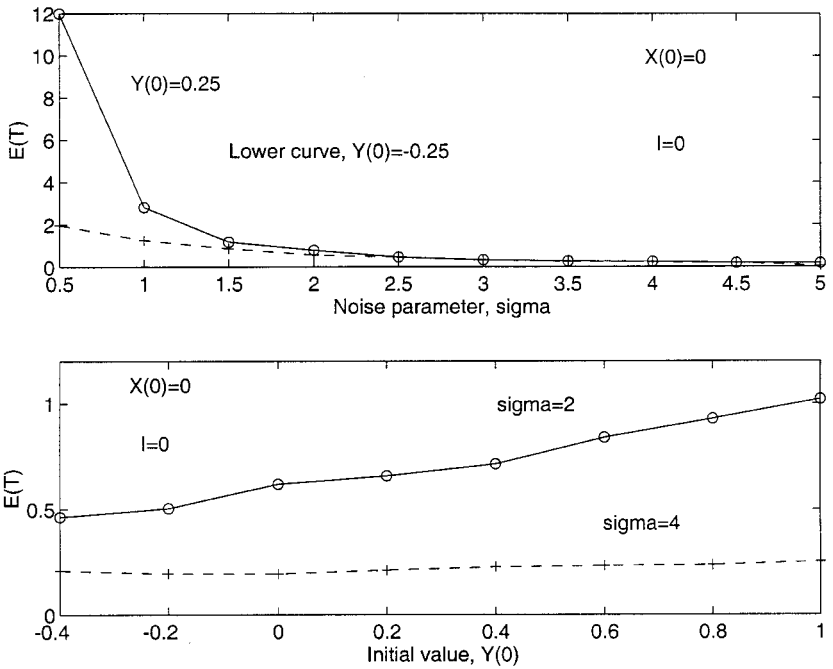


Figure 8: Effects of changing the initial value of the recovery variable  $Y(0)$  are illustrated for a fixed value of  $X(0) = 0$ . (Top) For the indicated values of  $Y(0)$ , the variation of the mean time to a spike as a function of noise parameter  $\sigma$  is shown. (Bottom) Variations in mean time to a spike as the initial value  $Y(0)$  changes for the two indicated values of the noise parameter.

in the top part of this figure with those in Figures 2 and 3 indicates that the variation in this mean as the noise parameter varies from 0.5 to 5.0 is similar for the three different values of  $X(0)$  even despite the different values of  $I$  and the fact that Figures 2 and 3 correspond to the periodic firing mode with a different value for  $Y(0)$ . That the mean time to a spike is moderately sensitive to changes in  $X(0)$  for fixed values of all the parameters and  $Y(0)$  can be seen in the lower part of Figure 7. Similar remarks apply to the effects of changing  $Y(0)$ , as can be gleaned from inspection of Figure 8. Noticeable here, however, is that when  $\sigma = 4$ , the mean time to a spike increases only gradually as  $Y(0)$  increases from  $-0.4$  to  $1.0$ .

In summary, we have investigated for the first time the determination of times for a threshold crossing in a nonlinear stochastic neuronal model, that of Fitzhugh-Nagumo, with the addition of a white gaussian noise representing stochastic excitation and inhibition. We have found moments of threshold crossing times accurately by solving the associated partial differ-

ential equations, obtained from the theory of Markov processes. The validity of the methods employed has been verified by comparison with computer simulation results. An interesting structure in the mean first passage time was noted at small values of the noise parameter. In future work, we will report our findings for the more complicated Hodgkin-Huxley system.

## Acknowledgments

---

H. C. T. appreciates support from the Riken Brain Science Institute, Saitama, Japan.

## References

---

- Burns, B. D. (1968). *The uncertain nervous system*. London: Arnold.
- Feng, J-F., & Brown, D. (2000). Integrate-and-fire models with nonlinear leakage. *Bulletin of Mathematical Biology*, *62*, 467–481.
- Konig, P., Engel, A. K., & Singer, W. (1996). Integrator or coincidence detector? The role of the cortical neuron revisited. *Trends in Neurosciences*, *19*, 130–137.
- Kreiter, A. K., & Singer, W. (1996). Stimulus-dependent synchronization of neuronal responses in the visual cortex of the awake macaque monkey. *Journal of Neuroscience*, *16*, 2381–2396.
- Lee, S-G., & Kim, S. (1999). Parameter dependence of stochastic resonance in the stochastic Hodgkin-Huxley neuron. *Phys. Rev. E*, *60*, 826–830.
- Liley, D. T. J., Alexander, D. M., Wright, J. J., & Aldous, M. D. (1999). Alpha rhythm emerges from large-scale networks of realistically coupled multi-compartmental model cortical neurons. *Network: Comput. Neural Syst.*, *10*, 79–92.
- Massanes, S. R., & Vicente, C. J. P. (1999). Nonadiabatic resonances in a noisy Fitzhugh-Nagumo neuron model. *Phys. Rev. E*, *59*, 4490–4497.
- Nozaki, D., & Yamamoto, Y. (1998). Enhancement of stochastic resonance in a Fitzhugh-Nagumo neuronal model driven by colored noise. *Phys. Lett. A*, *243*, 281–287.
- Plesser, H. E., & Gerstner, W. (2000). Noise in integrate-and-fire neurons: From stochastic inputs to escape rates. *Neural Computation*, *12*, 367–384.
- Plesser, H. E., & Tanaka, S. (1997). Stochastic resonance in a model neuron with reset. *Physics Letters A*, *225*, 228–234.
- Rodriguez, R. (1995). Coupled Hodgkin-Huxley neurons with stochastic synaptic inputs. In J. Bertrand (Ed.), *Modern group theoretical methods in physics* (pp. 233–242). Norwood, MA: Kluwer.
- Shadlen, M. N., & Newsome, W. T. (1995). Noise, neural codes and cortical organization. *Curr. Opin. Neurobiol.*, *4*, 569–579.
- Softky, W. R., & Koch, C. (1993). The highly irregular firing of cortical cells is inconsistent with temporal integration of random EPSPs. *J. Neurosci.*, *13*, 334–350.
- Stevens, C. F., & Zador, A. M. (1998). Input synchrony and the irregular firing of cortical neurons. *Nature Neuroscience*, *1*, 210–217.



- Tanabe, S., & Pakdaman, K. (2001). Dynamics of moments of Fitzhugh-Nagumo neuronal models and stochastic bifurcations. *Phys. Rev. E*, *63*, 031911.
- Tiesinga, P. H. E., José, J. V., & Sejnowski, T. J. (2000). Comparison of current-driven and conductance-driven neocortical model neurons with Hodgkin-Huxley voltage-gated channels. *Phys. Rev. E*, *62*, 8413–8419.
- Tuckwell, H. C. (1976). On the first exit time problem for temporally homogeneous Markov processes. *J. Appl. Prob.*, *13*, 39–48.
- Tuckwell, H. C. (1986). Stochastic equations for nerve membrane potential. *J. Theoret. Neurobiol.*, *5*, 87–99.
- Tuckwell, H. C. (1989). *Stochastic processes in the neurosciences*. Philadelphia: SIAM.
- Tuckwell, H. C., & Rodriguez, R. (1998). Analytical and simulation results for stochastic Fitzhugh-Nagumo neurons and neural networks. *J. Computational Neuroscience*, *5*, 91–113.
- Wan, F. Y. M., & Tuckwell, H. C. (1982). Neuronal firing and input variability. *J. Theoret. Neurobiol.*, *1*, 197–218.

---

Received August 24, 2001; accepted July 3, 2002.